Proceedings of the Korea Nuclear Society Spring Meeting

Pohang, Korea, May 1999

An Observation of Single Bubble Growth and Departure on a Microscale Heater Array

Sungwon Bae[2], Jungho Kim[1], and Moohwan Kim[2]

[1]University of Maryland

Department of Mechanical Engineering College Park, MD 20742, USA, Phone: +1-(301) 405-5437

[2]Pohang University of Science and Technology

Department of Mechanical Engineering, Pohang City, Kyungbuk, 790-784 Korea, Phone: +82-(0562)-279-2165

ABSTRACT

The objective of this work is measure space and time resolved heat transfer variations during nucleate pool boiling of FC-72 using a micro-scale heater array in conjunction with a high speed CCD. The feedback loops used in this work are vast improvements over those used in previous work, and are described here in detail. The heater array is constructed using VLSI techniques, and consists of 96 serpentine platinum resistance heaters on a quartz substrate. Electronic feedback loops are used to keep the temperature of each heater in the array at a specified value, and the variation in heater power required to do this is measured. Data are obtained with the bulk liquid subcooled by 2 °C at a system pressure of 0.8 atm. Isolated bubbles are obtained at a wall superheat of 29 °C. One nucleation site occurred in the middle of a 2 x 2 array of heaters and at least three heater lengths away from other bubbles. The heat transfer variation vs. time from the four heaters directly around this nucleation site is plotted and correlated with images of the bubble obtained using the high speed CCD. It is revealed that there are other major heat transfer mechanisms in addition to the microlayer evaporation, which has been thought to be the dominant heat transfer mechanism in saturated pool boiling. The purpose of this paper is to provide a description of the experimental technique and demonstrate the technology.

1. INTRODUCTION

Convective nucleate boiling heat transfer is major heat transfer mechanism between fuel rod and primary loop water of pressurized water reactor system in nuclear power plant. In order to predict the nucleate boiling heat flux in pool boiling situation as well as convective situation, it is most important to interpret the relationships between bubble behavior and heat flux. Much work has been performed over the past forty years to try to clarify boiling heat transfer mechanisms, some of which are described below. One mechanism was proposed by Forster and Zuber [1], and is called microconvection. The bubble motion during growth causes a nominally radial velocity field to form that causes enhanced forced convection around the site. Another mechanism, commonly termed liquid-vapor exchange [2], occurs when the departing bubble's volume is replaced by bulk liquid resulting in an enhanced convective effect. A third mechanism, often termed microlayer evaporation, is associated with evaporation of a thin liquid

layer that forms underneath the bubble during the early stages of bubble growth. The existence of the microlayer was first hypothesized by Snyder and Edwards [3]. Transient conduction to the liquid is another heat transfer mechanism that occurs after the bubble "scavenges" the thermal boundary layer from the wall. Many models have been proposed that incorporate some of the above mechanisms as well as others. For example, Han and Griffith[4] developed a combined nucleate boiling model in which the vapor-liquid exchange and transient conduction concept were included.

The amount of heat transferred by these small-scale, transient mechanisms are difficult to quantify and the extension to macroscopic calculations of area and time-averaged heat transfer requires knowledge of the number and size distribution of nucleation sites along with the frequency of the bubble generation. In order to interpret nucleate boiling heat transfer mechanisms from a microscopic viewpoint, it is necessary to analyze the heat transfer behavior of a single bubble. The micro-scale heater array was adapted in this work for that purpose since it has high temporal and spatial resolution in contrast to conventional measuring devices. In addition to this highly resolved heat transfer data, visual information was obtained to enable correlation between the heat transferred from the wall and the bubble dynamics. A description of this experimental technique along with some results was described by Rule and Kim [5] and Rule, Kim, and Kalkur [6]. Since this work, a second generation feedback loop board was constructed that provides superior performance and which is much more user friendly. The purpose of this paper is to provide a description of the newer experimental technique and a demonstration of this technology.

2. EXPERIMENTS

2.1. Micro-scale Heater

The micro-scale heater is made constructed on a transparent quartz substrate using VLSI techniques similar to those described in Rule, Kim, and Kalkur [6]. First, a Ti/Pt layer is deposited using thermal evaporation-deposition. Second, a photomask is used to etch the Ti/Pt into the desired pattern. Next, a layer of aluminum is deposited onto the surface and etched to construct power leads. About eight chips can be constructed on a single quartz wafer. The wafer is diced to obtain the individual chips, and each chip is mounted in a Pin Grid Array. A photograph of an array of 96 heaters is shown on **Figure** 1 along with bubbles nucleating on the array. Each heater in the array is 0.27 mm x 0.27 mm in size. The heaters have a nominal resistance of 1000 Ω and a nominal temperature coefficient of resistance of 0.002 °C^{-1}.

2.2. Electronic Feedback Circuit

The temperatures of the heaters in the array are kept at constant temperature by an array of 96 feedback circuits similar to those used in constant-temperature hot-wire anemometry. A schematic of one of these circuits is shown on **Figure** 2. The heater represents one resistance in a Wheatstone bridge. The op-amp senses any imbalance in the bridge and outputs whatever voltage necessary to bring the bridge back into balance. A chopper stabilized op-amp (LTC1150 CN8-ND) was used in the feedback loops because they exhibit extremely small input offset voltages as wells as low drift with temperature. The heater resistance, and therefore the heater temperature, can be controlled by varying the resistance of a digital potentiometer made by Dallas Semiconductor (DS1267010). This chip consists of two 10 kΩ digital potentiometers, each having 256 wiper positions. The two potentiometers in this chip are connected in series to make a single 20 kΩ potentiometer with 512 wiper positions. Control of the wiper position is performed through a 3-wire serial interface to a PC and digital I/O card. The digital potentiometer is connected in parallel with a 50 kΩ resistor. For the resistor values indicated in **Figure** 2, a heater of nominally 1000 Ω resistance can be varied over a 350 Ω range. Because the heaters have a temperature coefficient of resistance of nominally 0.002 °C^{-1}, the temperature of the heater can be varied by about 175 °C. Since the

digital potentiometer has 512 settings, the temperature of the heaters can be changed in 0.34 °C increments. Sixteen of these circuits are constructed on a single card. Six of these cards plug into a custom designed motherboard which routes the signals from the digital I/O card to the individual feedback loops.

2.3. Data Acquisition System

The data acquisition system is a custom designed unit that is capable of sampling 16K data points from each heater at speeds up to 10 kHz with 12 bits of resolution. Data acquisition is triggered by the rising edge of TTL signal, and continued until the 16K buffers are full. Once the data acquisition is complete, the data contained in the buffers are downloaded to the computer using a digital I/O card. Complete details of the data acquisition system are provided in Rule, Kim, and Kalkur [6].

2.4. Boiling Rig

Figure 3 shows a schematic of a boiling rig that was made available to the authors by NASA. An aluminum chamber 120 mm in diameter and 100 mm in height, serves as a boiling chamber. Thermofoil heaters (OMEGA) attached to the outside of this chamber are used to heat the fluid in the chamber. A K-type thermocouple within the chamber along with a temperature controller is used to keep the fluid at the desired temperature. Two pressure transducers are used to measure the air chamber and boiling chamber pressures. A bellows is used to control the pressure of the system by pressurizing the air side of the boiling chamber. A 3mm thick teflon spacer is used to reduce thermal conduction through the heater rig wall to the upper structure. The bulk fluid is degassed by repeatedly pulling a vacuum on the fluid so that the dissolved gas concentration is below 0.0001 mole/mole. The fluid used is FC-72 and properties are tabulated in Table 1.

2.5. High Speed Digital Camera

The semi-transparent nature of the heater array enables images to be made of the bubbles growing on the surface from below using a high-speed CCD camera (SpeedCam 512). This camera has a maximum frame rate of 1000 frame per second with 512 x 512 resolution. A microscope lens (Infinity Optical KC Lens with IF-4 objective) is used to magnify the small image of the heater array. Visual recording is triggered using the same signal used to trigger the data acquisition system, allowing heat transfer measurements and visual records to be made simultaneously. The data acquisition system and digital video recorder were found to be synchronized within 1 ms (1 frame) over the entire data acquisition time.

3. HEATER CALIBRATION

The heater array was calibrated in an insulated, circulating, constant temperature oil bath which is held within 0.2 °C of the calibration temperature. An impinging jet of heated oil onto the heater provides a high heat transfer coefficient. Calibration consists of finding the digital potentiometer wiper position that causes the feedback loop to begin regulating for a given oil bath temperature. **Figure** 4 shows the voltage across a few heaters as the wiper position on the digital potentiometer is increased for a fluid temperature of 75 °C. A sharp increase in the output voltage occurs once the op-amp begins to regulate. The uncertainty in threshold wiper position is about 2 positions, or about 0.7 °C in heater temperature. In practice the wiper positions for each heater are initially set to a very low value (about 10) and the output voltages of the circuits (the voltages at position A on **Figure** 2) are measured. These voltages represent the baseline voltages across the heaters without the op-amps regulating. Threshold voltages for the calibration are obtained by adding 3 mV to these baseline voltages. In the actual calibration, the wiper positions are incremented and the wiper position that results in the

output voltage exceeding the threshold voltage is recorded. Repeated calibration of the heaters at a given temperature resulted in calibrations that differed no more than 1 wiper position, indicating that both the bath temperature and the electronics were stable. Calibration of the heaters were performed at temperatures between 50 °C to 95 °C in 5 °C increments.

4. DATA REDUCTION

The quantity of interest is not the total heat supplied to a given heater, but the heat supplied from that heater to the fluid. A portion of the total heat supplied to a heater is transferred to the liquid either by single phase or two phase convection, and a portion is conducted through the substrate. This substrate conduction needs to be measured and subtracted from the total heat supplied to obtain the heat transfer from the wall to the fluid. The substrate conduction at each wall temperature can be determined by pressurizing the test rig to suppress nucleation and measuring the heat transfer from each heater under these conditions. Because there is no boiling, the substrate is cooled by substrate conduction and natural convection. The substrate conduction can be obtained by subtracting the natural convection from the total heat transfer from the heater. Eq.(1) represent the correlation used to quantify the natural convection from heater array [7].

$$Nu = 0.54 Ra_L^{1/4} \qquad (10^4 < Ra_L < 10^7) \tag{1}$$

The Rayleigh Number is calculated as follows.

$$Ra_L = \frac{g\beta}{\alpha\nu} L^3 \left(T_w - T_\infty\right) \tag{2}$$

The length scale L represents the hydraulic diameter of heater array. For an array 2.7 x 2.7 mm, L is computed to be 79.5 μm. It should be noted that the natural convection computed from the above equation is the average heat transfer over the entire heater. The substrate conduction, however, is measured from each heater in the array. The results for a bulk pressure of 2.72 atm are shown on **Figure** 5. Because the heater temperature is held at constant temperature, the value of substrate conduction for each individual heater is independent of the state of the fluid (boiling or natural convection) above the surface. At a wall temperature of 80 °C, the average natural convection across the array is computed to be 1.3 W/cm^2. The average substrate conduction over the array is measured to be 2.0 W/cm^2, with lower values toward the center of the array and higher values toward the edge of the array, as expected. The accuracy of the natural convection correlation directly affects the calculation of substrate conduction.

4.1. Uncertainty Analysis

The uncertainty in total heat fluxes is relatively small since it is computed directly from the measured voltage across the heaters. The uncertainty in natural convection is taken to be 100% since significant variations can occur across the array. An uncertainty of about 10% in substrate conduction is assumed since the heat transfer coefficient around the heater during boiling increases above that associated with natural convection, and this can change the value of substrate conduction calculated from the pressurized experiment. The final uncertainty in the heat flux traces below was calculated according to the method of Kline and McClintock [8] to be 2.1W/cm^2 when the surface is set to 80 °C. The instantaneous voltage required to keep each heater at a constant temperature is measured and used to calculate power as follows.

$$q''_{nb,i} = \left(\frac{V_{avg,i}^2}{R_i A_i} - q''_{sc,i} A_i \right) / A_i \tag{3}$$

The heater resistance is corrected to account for the resistance-temperature coefficient of platinum. Because all the heaters in the array

are essentially at the same temperature, heat conduction between adjacent heaters is negligible.

5. RESULTS

5.1. Boiling Curve

The boiling curve shown on **Figure** 6 was generated by decreasing the temperature of the heaters from 95 °C to 50 °C in 5°C increments. Boiling curves with increasing wall temperature were not obtained because of incipience problems at low temperatures. The heat flux is the average heat flux over the entire array. Boiling was observed at temperatures above 65 °C. Two runs were made, and the data is seen to be quite repeatable.

5.2. Nucleate Boiling Heat Flux

Shown on **Figure** 7 are the heat flux traces for heaters 15, 16, 34, and 35 (see **Figure** 1 for the location of these heaters) at a wall temperature of 80 °C. The other heaters around this bubble showed little variation in heat flux. A single bubble was observed to grow and generate regularly from a site underneath these heaters with a departure frequency of about 90 Hz. Shown on **Figure** 8 is the state of the bubble over one bubble departure cycle between 0.083 s to 0.095 s. The times noted on **Figure** 8 correspond to those on **Figure** 7. Between 0.084 and 0.085 s, nucleation of a new bubble occurs-this event is associated with a sharp increase in heat flux. The average heat flux over the 4 heaters increases from about 2.2 W/cm^2 to 3.5 W/cm^2 during nucleation. What appears to be dry spot on the surface grows to maximum size at 0.086 s, then this begins to shrink until bubble departure at between 0.089 s and 0.091 s. Unfortunately, the visualization data at 0.090 s was not available due to improper digitization when downloading the data from the SpeedCam to the computer. Although the dry spot decreases in size between 0.086 s and 0.091 s, the overall radius of the bubble increases as more and more vapor is added to the bubble. At 0.089 s, the bubble departs from the surface and the shadow of the departing bubble is observed. **Figure** 9 shows the accumulated heat flux normalized on the total heat transferred to the bubble from the heater (24.2 W/cm^2). It is seen that the almost 65% of the total heat is transferred from the time the dry spot reaches a maximum value to the bubble departure time. This result indicates that the principal method of heat transfer may be evaporation of fluid near the contact line as liquid rewets the wall before bubble departure. Although the maximum heat transfer rates are observed during bubble growth, the short time requiredto bubble growth results in relatively little heat being transferred. This mechanism is different from the widely accepted view that microlayer evaporation is the dominant heat transfer mechanism in saturated pool boiling.

6. CONCLUSION

A technique whereby spatially and temporally resolved heat fluxes can be measured during boiling has been documented and demonstrated. This technique has the potential to provide significantly more information regarding boiling heat transfer mechanisms than has been obtained using techniques to date.

ACKNOWLEDGEMENT

This work has been performed when Mr. Bae visited the University of Denver. Special thanks should be given to AFERC in POSTECH, and to Mr. J.D.Quaine, the research assistance in University of Denver.

NOMENCLATURE

A	Area [cm^2]
g	Gravitational acceleration [m/s^2]
L	Length Scale [m]
Nu	Nusselt number [non-dimensional]
R	Resistance [Ω]
Ra_L	Rayleigh number [non-dimensional]
T	Temperature [°C, K]
$q"$	Heat flux [W/cm2]

Subscript

avg	*average*
i	*index of heater*
nb	*nucleate boiling*
w	*wall*
sc	*substrate conduction*
¥	*bulk*

Greek Letters

a	Thermal diffusivity [m^2/s]
b	Volume expansion coefficient [$°C^{-1}$]
ν	Kinematic viscosity [m^2/s]

REFERENCES

1. Forster, H.K., and Zuber, N., Growth of a Vapor Bubble in a Superheated Liquid, Journal of Applied Physics, 25, p.474, 1954.

2. Hsu, Y.Y., and Graham, R., An Analytical and Experimental Study of the Thermal Boundary Layer and Ebullient Cycle in Nucleate Boiling, NASA Rept. TN-D-594, 1961.

3. Snyder, N.W., and Edwards, D.K., Summary of Conference on Bubble Dynamics and Boiling Heat Transfer, JPL memo 20-137, Jet Propulsion Laboratory, California Institute of Technology, 1956.

4. Han, C.Y., and Griffith, P., The Mechanism of Heat Transfer in Nucleate Pool Boiling-Part I, Int. J. Heat Mass Transfer, 8, pp.887-904, 1965.

5. Rule, T.D. and Kim, J., Wall Heat Transfer Measurements in Saturated Pool Boiling of FC-72 on a small Heated Area, Proceedings of the ASME IMECE Conference, Dallas, TX, 1997.

6. Rule, T.D., Kim, J., and Kalkur, T.S., Design, Construction and Qualification of a Microscale Heater Array for Use in Boiling Heat Transfer, NASA/CR-1998-207407, 1998.

7. Lioyd, J.R., and Moran, W.R., Natural Convection Adjacent to Horizontal Surface of VariousPlanforms , ASME Pap. 74-WA/HT-66, 1974.

8. Kline, S.J. andMcClintock, F.A., Describing Uncertainties in Single-Sample Experiments, Mechanical Engineering, Vol 75, pp.3-8, 1953.

Table 1. The transport and thermodynamic properties of FC-72 at 52.6 °C

Property name	Value
Density of liquid	1.6821×10^{3} kg/m^3
Density of vapor	11.5 kg/m^3
Thermal conductivity	5.7113×10^{-2} W/mK
Specific heat	1.0467×10^{3} J/kgK
Viscosity	6.8618×10^{-4} kg/ms
Thermal expansion coefficient	1.620×10^{-3} °C^{-1}
Thermal diffusivity	3.2439×10^{-8} m^2/s
Kinematic viscosity	4.0793×10^{-7} m^2/s
Surface tension	0.884 N/m

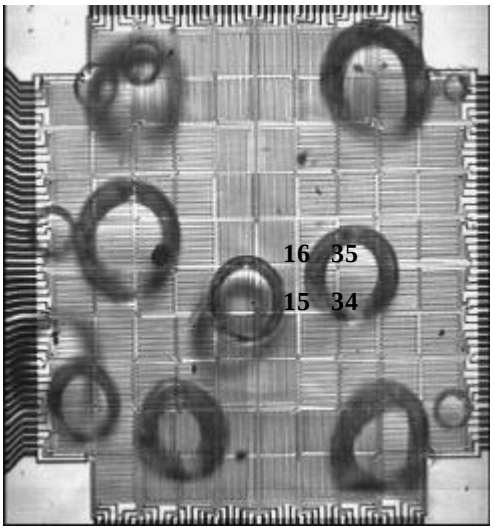

Figure 1. Photograph of the square arranged 96 heaters

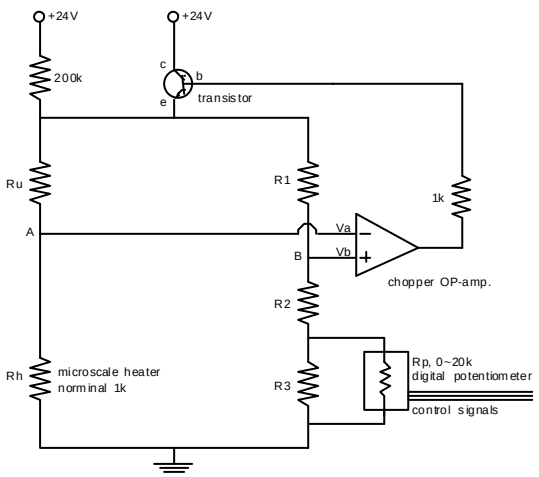

Figure 2. Schematic of the heater feedback control circuit

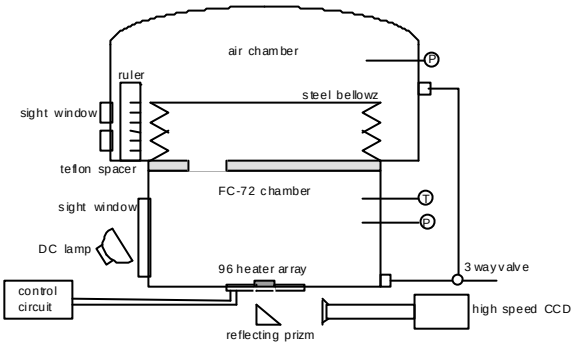

Figure 3. Schematic diagram of the main heater experiment facility

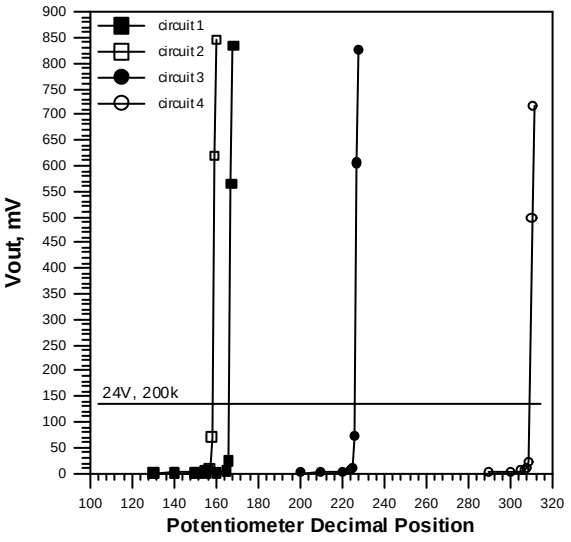

Figure 4. Circuit regulation curves for four feedback circuits in the heater array; Surface temperature=75 °C

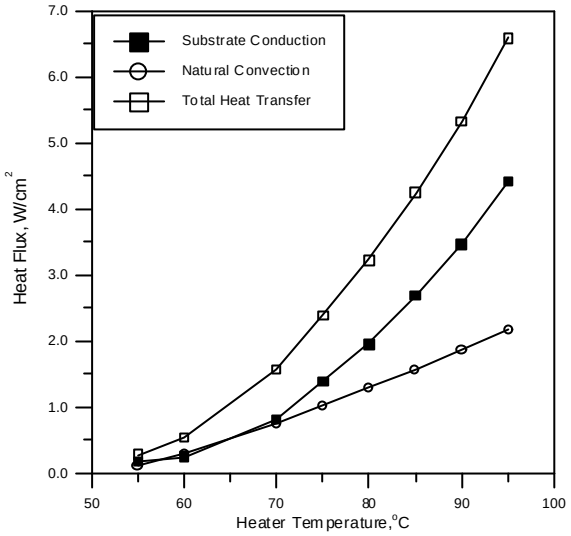

Figure 5. Result of 3 atm pressurized experiment

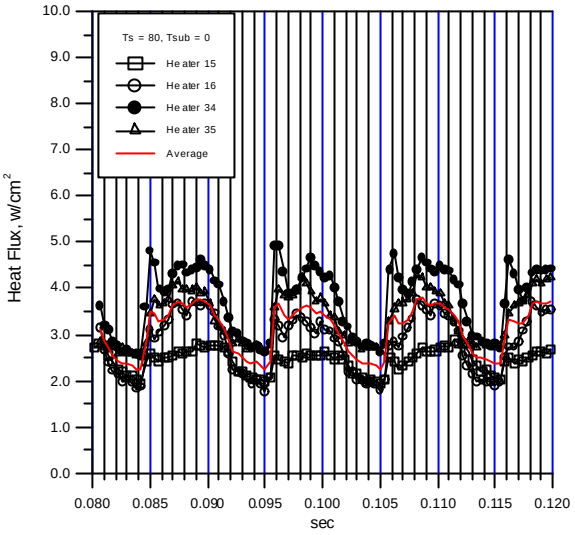

Figure 7. Nucleate boiling heat flux during some periodic cycles of bubble

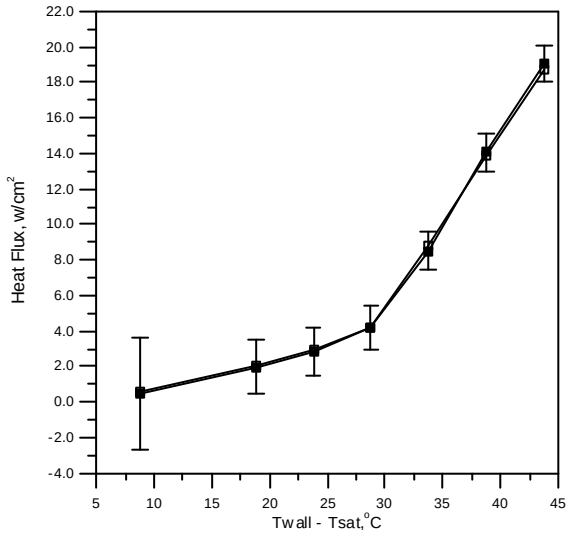

Figure 6. Incipient region boiling curve for saturation pool boiling of FC-72

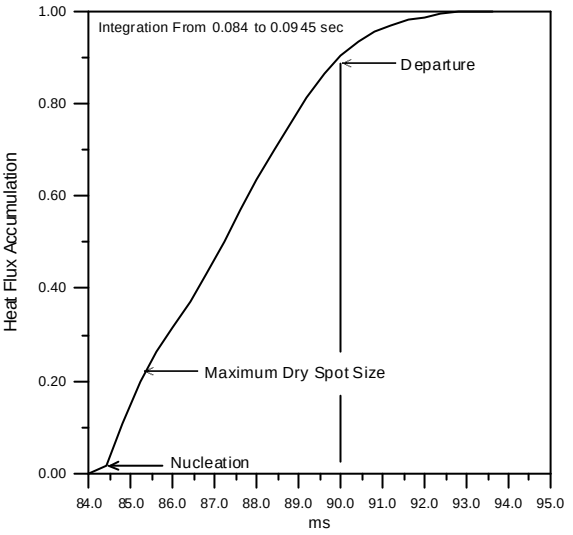

Figure 9. Accumulated heat flux during one bubble cycle normalized to the total heat transferred

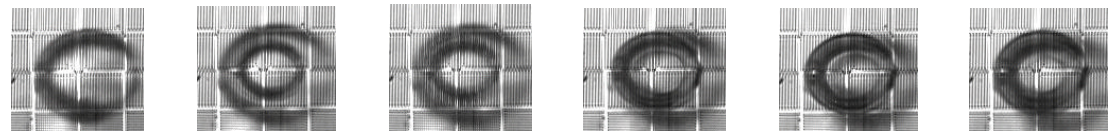

(a) 0.084 (b) 0.085 (c) 0.086 (d) 0.087 (e) 0.088 (f) 0.089

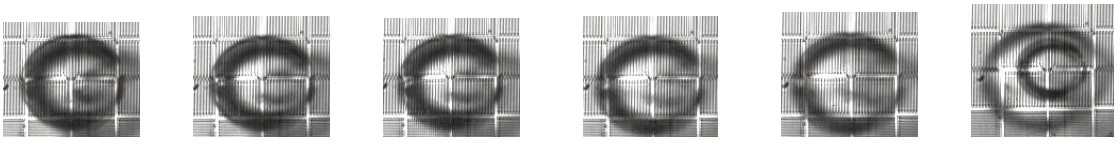

(g) 0.091 (h) 0.092 (i) 0.093 (j) 0.094 (k) 0.095 (l) 0.096

Figure 8. Photographic image of bubble triggered to the heat flux data in Figure 7